

Measurements of $\gamma\gamma$ and $\gamma+b$ cross sections

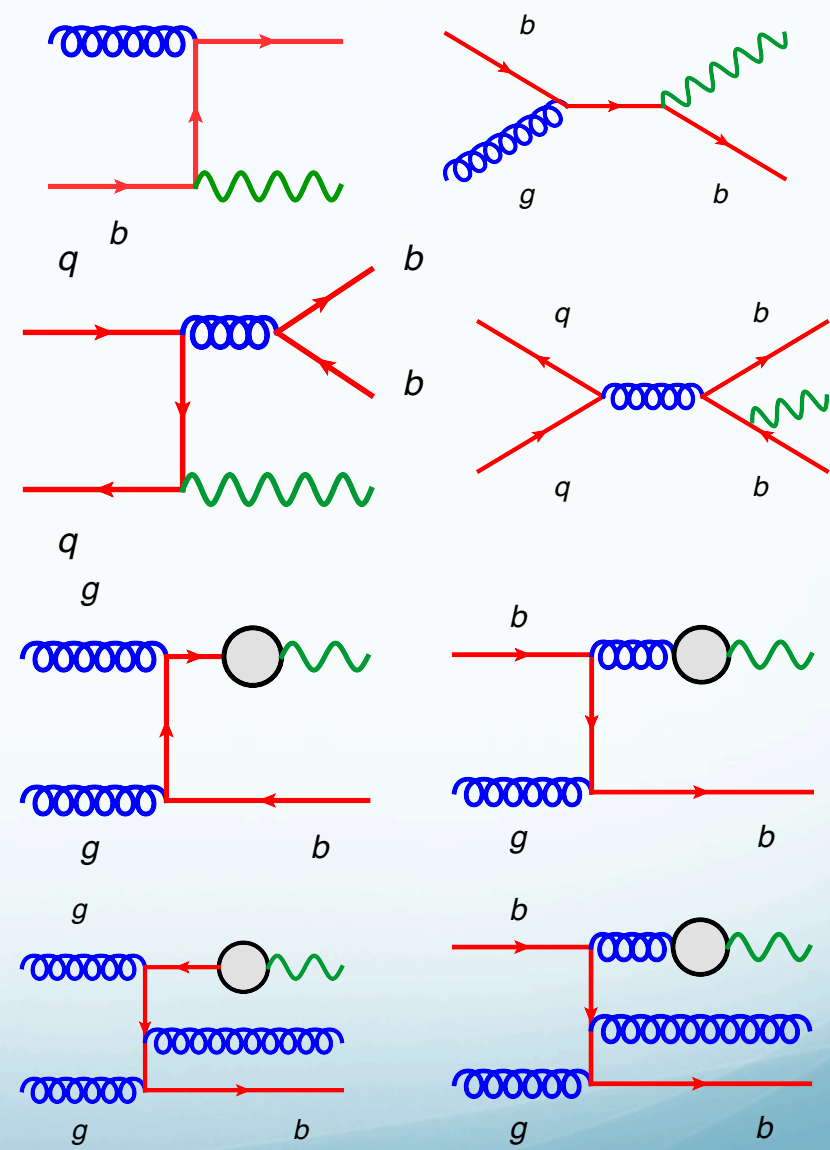
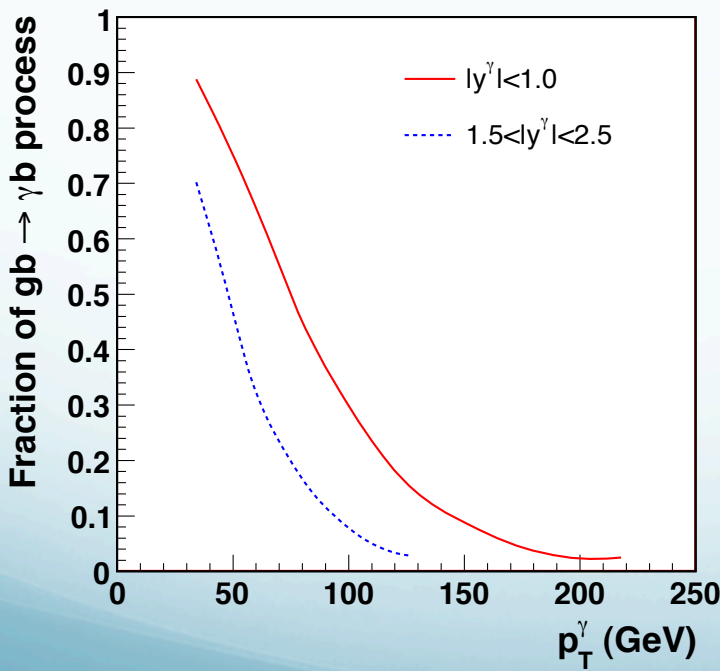
P. Svoisky, for the D0 Collaboration

Motivation

- Both $\gamma\gamma$ and $\gamma+b$ use high energy resolution of a photon
- $\gamma+b$ probes a wide range of proton momentum fractions $0.007 < x < 0.4$
 - Excellent for tuning b-quark and gluon PDFs
 - Gluon to bb fragmentation
- $\gamma\gamma$ spectrum is an indicator of high energy states
 - One has been just announced
 - Precise cross section measurements
 - New physics still possible at even higher energies
 - Kaluza-Klein gravitons, extra dimensions, etc.

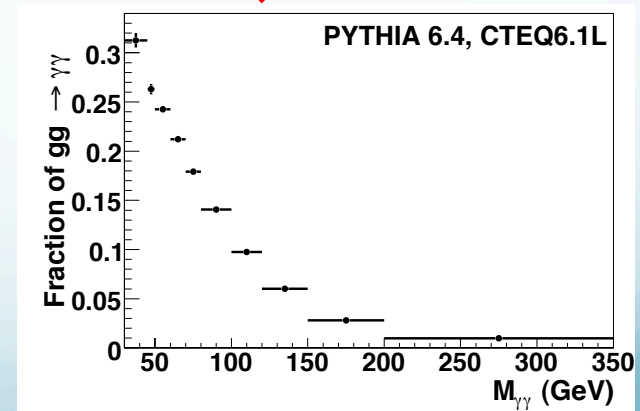
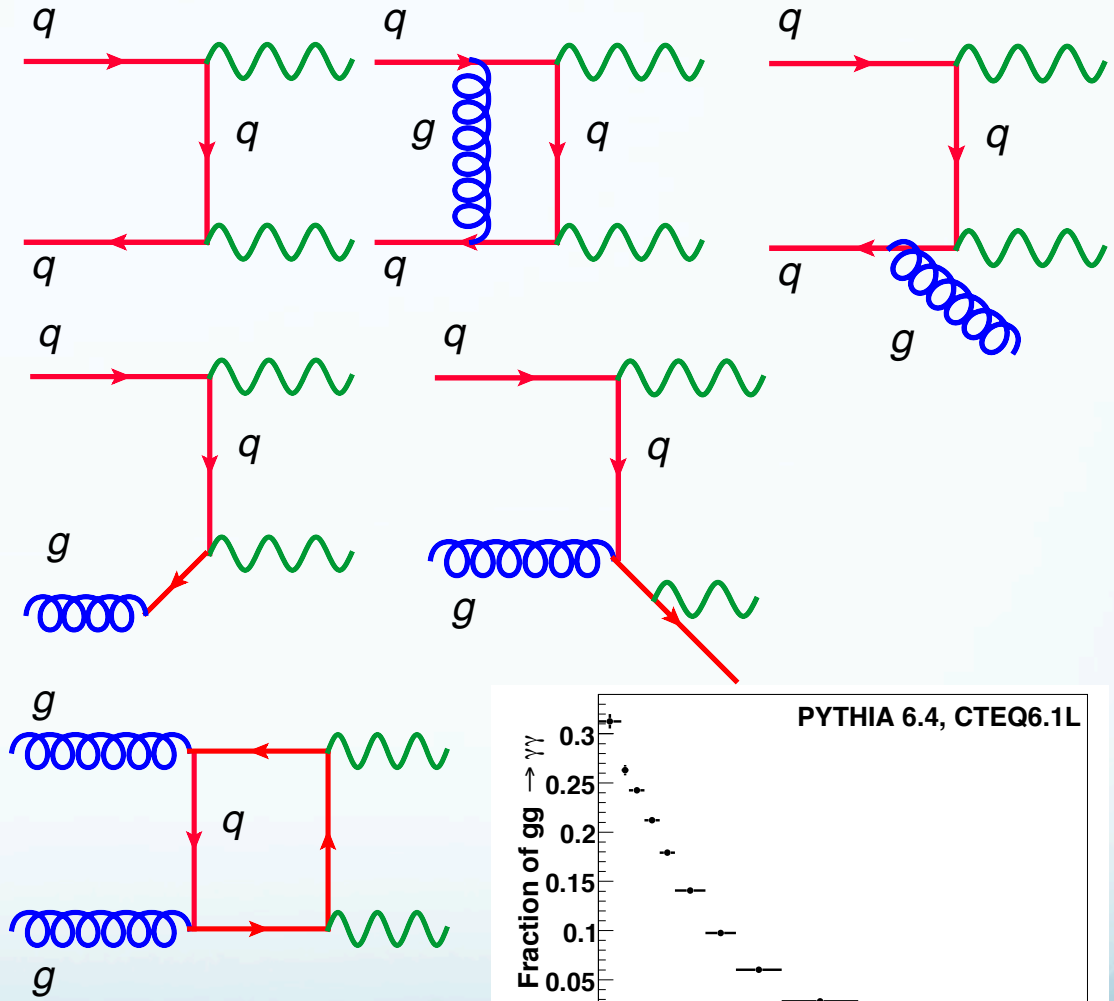
$\gamma + b$ theory

- Compton-like scattering at low p_T^γ
- Quark annihilation at high p_T^γ
- Higher order fragmentation processes
 - Gluon fusion
 - Corrections



Direct QCD $\gamma\gamma$

- Leading process at Tevatron is Born ($q\bar{q} \rightarrow \gamma\gamma$)
 - At NLO real emissions and virtual corrections
 - DIPHOX uses fixed order NLO for initial state radiation and fragmentation functions
 - Initial state corrections resummed to all orders of α_s in RESBOS to NNLL accuracy
- $qg \rightarrow \gamma\gamma$ (NLO)
 - Up to 50% at LHC energies
- Box diagrams (with corrections) NNLO but important at low mass (large gluon PDFs)



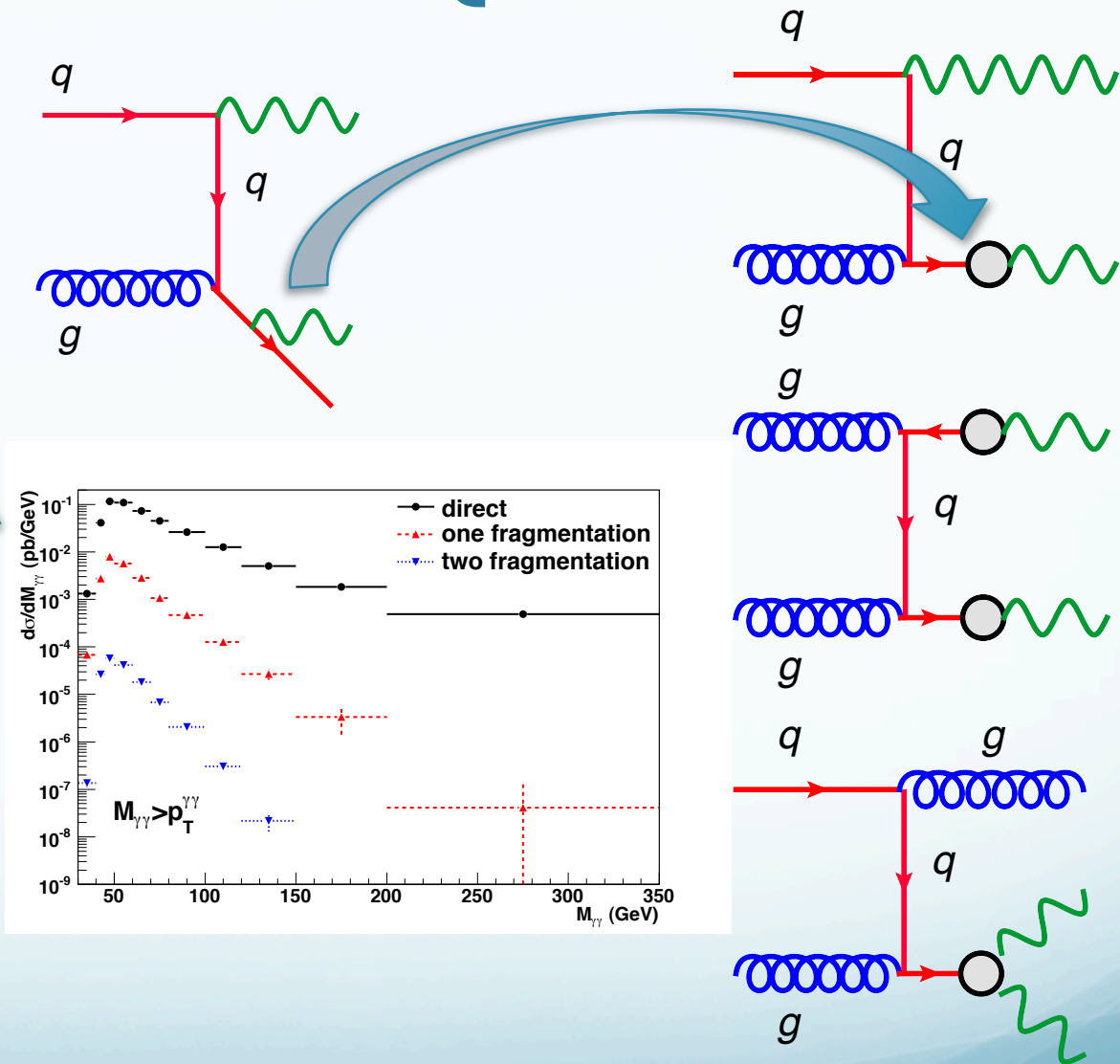
Fragmentation QCD $\gamma\gamma$

- Single or double fragmentation
 - Needs isolation to separate

$$E_T^{iso} = \sum_{i, R < 0.4} (p_{T,i} - p_{T,\gamma})$$

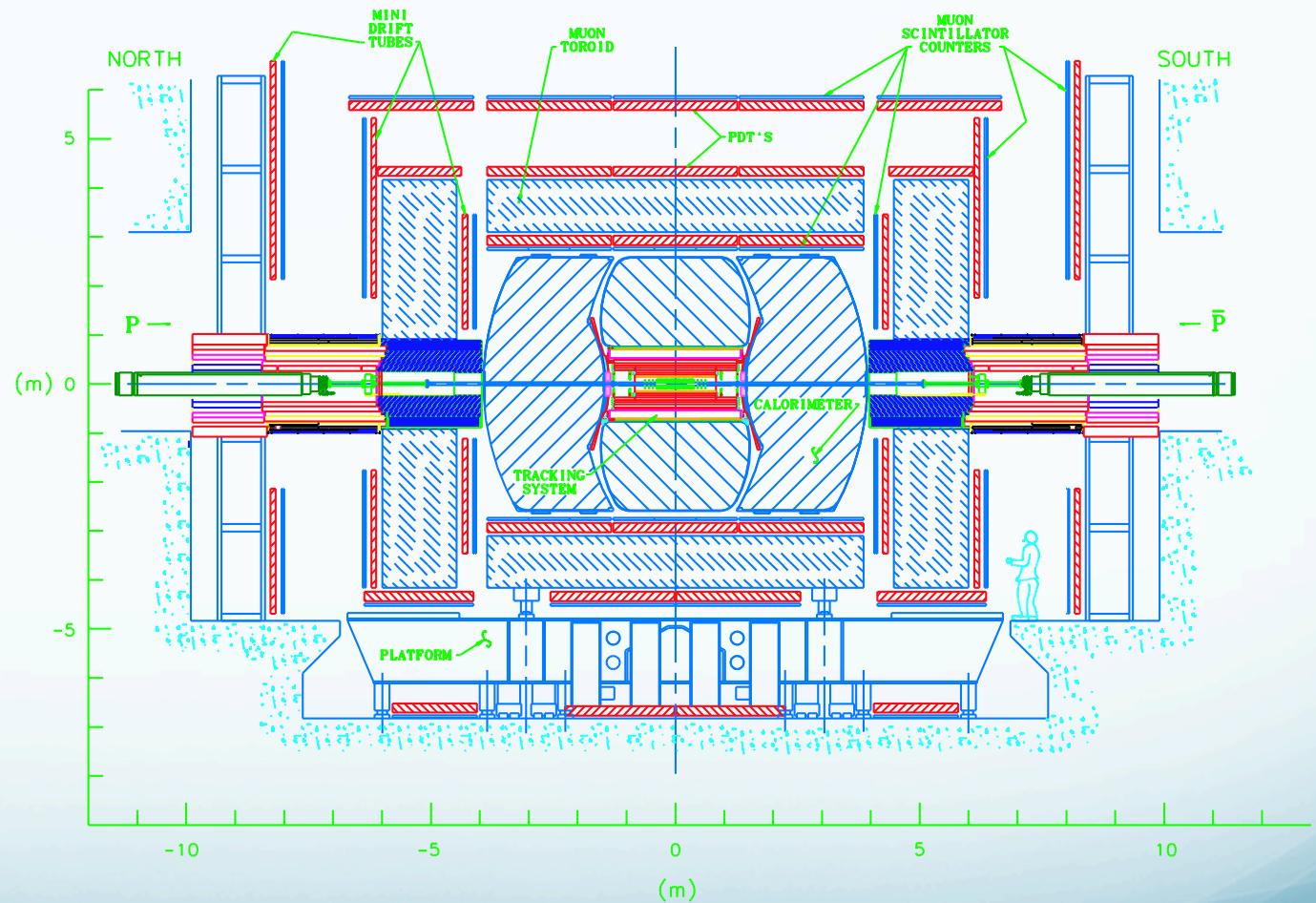
- $M_{\gamma\gamma} > p_T^{\gamma\gamma}$ removes a lot of fragmentation (low at Tevatron energies)

- Collinear singularities (final state)
 - Factorized into FF D (Z, μ) in DIPHOX
 - Auxiliary regulator in RESBOS $Q_T < E_T^{iso}$, single fragmentation is included via parametrization approximating NLO FF rates
 - Parton showers replaced by ME at scale Q SHERPA



D0 detector

- Liquid Ar calorimeter
- Silicon micro-strip tracker
- Central fiber tracker
- Muon system
- Central preshower

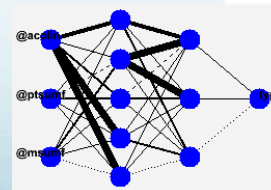
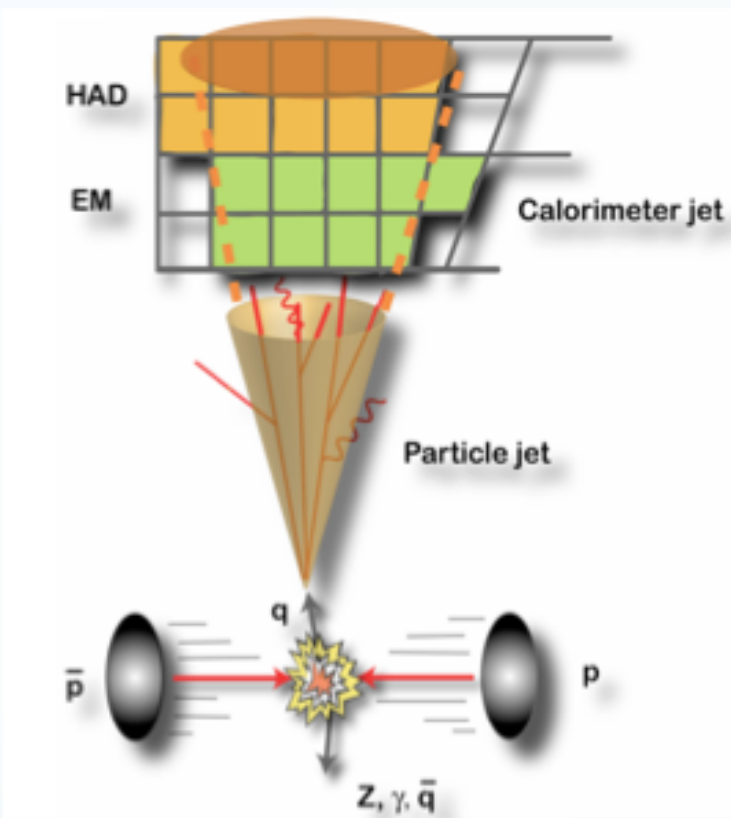


Analyses

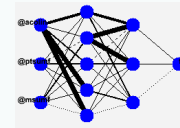
- $\gamma + b$ measuring $d\sigma/dp_T \gamma$
 - $|\eta_\gamma| < 1.0$ or $1.5 < |\eta_\gamma| < 2.5$
 - $|\eta_{b\text{-jet}}| < 1.5$, $p_T^{b\text{-jet}} > 15$ GeV
 - $L = 8.7 \pm 0.5$ fb $^{-1}$
- $\gamma \gamma$ measuring $d\sigma/dM_{\gamma\gamma}$, $d\sigma/dp_T \gamma\gamma$, $d\sigma/d\Delta\phi_{\gamma\gamma}$, $d\sigma/d|\cos\theta^*|$
 - $|\eta_\gamma| < 0.9$, $p_T^1 > 21$ GeV, $p_T^2 > 20$ GeV, $\Delta\phi_{\gamma\gamma} > \pi/2$
 - $M_{\gamma\gamma} > p_T \gamma\gamma$, $30 < M_{\gamma\gamma} < 350$ GeV, $p_T \gamma\gamma < 100$ GeV
 - $L = 4.2 \pm 0.3$ fb $^{-1}$
 - Also $d^2\sigma/dp_T \gamma\gamma dM_{\gamma\gamma}$, $d^2\sigma/d\Delta\phi_{\gamma\gamma} dM_{\gamma\gamma}$, $d^2\sigma/d|\cos\theta^*| dM_{\gamma\gamma}$ in 3 $M_{\gamma\gamma}$ bins

γ identification

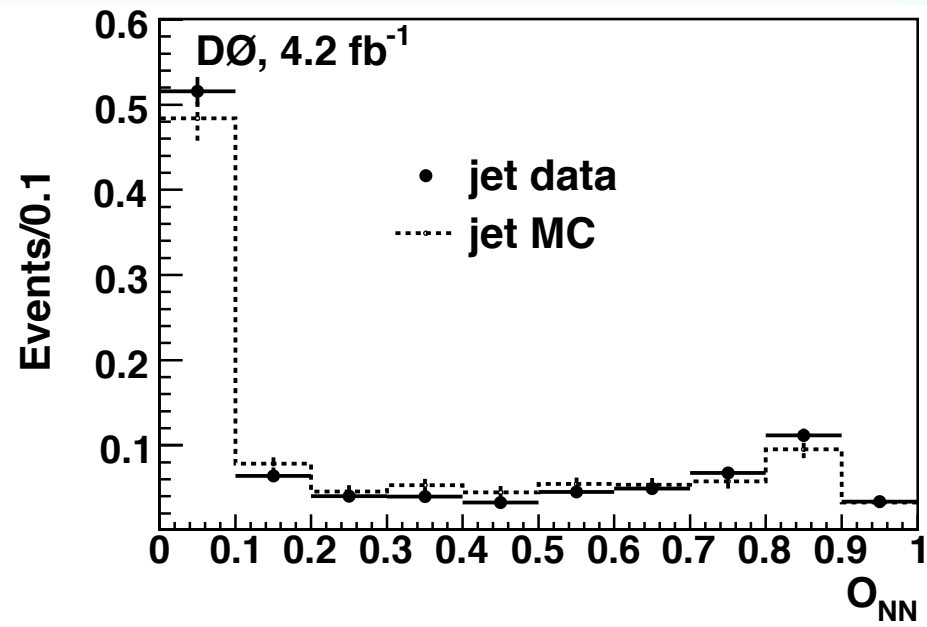
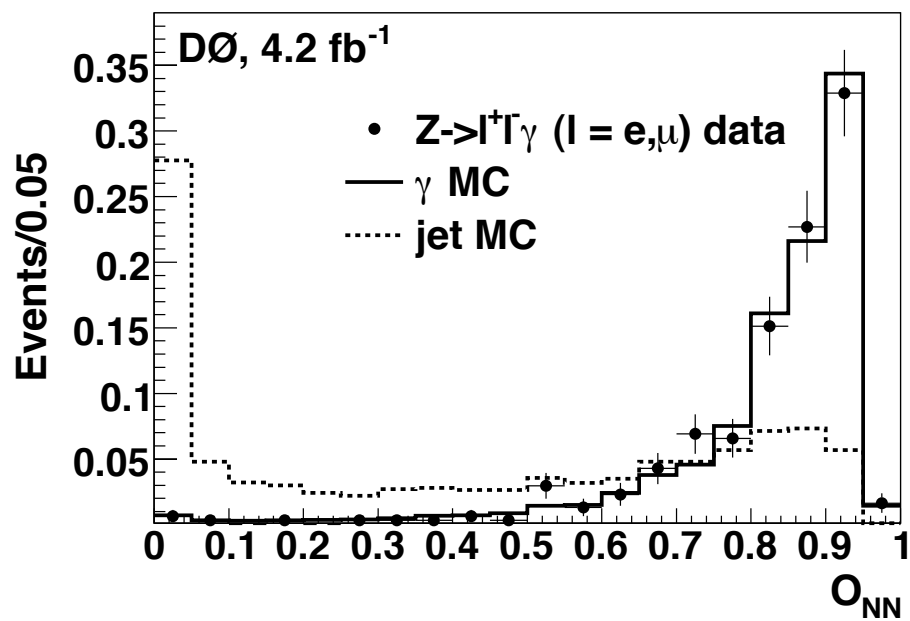
- $I_{\text{iso}} = [E_{\text{tot}}(0.4) \cdot E_{\text{EM}}(0.2)] / E_{\text{EM}}(0.2) < 0.07$ (calorimeter cone isolation)
- $\text{EMF} > 0.97$ (electro-magnetic fraction)
- $p_{T,\text{trk}}^{\text{iso}} = p_{T,\text{trk}}(0.4) \cdot p_{T,\text{trk}}(0.2) < 1.5 \text{ GeV}$ (track cone isolation)
- $\text{SigPhi} < 18$ (cell energy-weighted shower shape)
- $\text{TrkProb} < 0$ and $\text{HOR} < 0.9$ (anti-track match)
 - Track-match probability
 - Tracker hits along the projection from the calorimeter (hits on the road)
- $\text{ANN} > 0.3$ (Neural Net output)



γ ANN

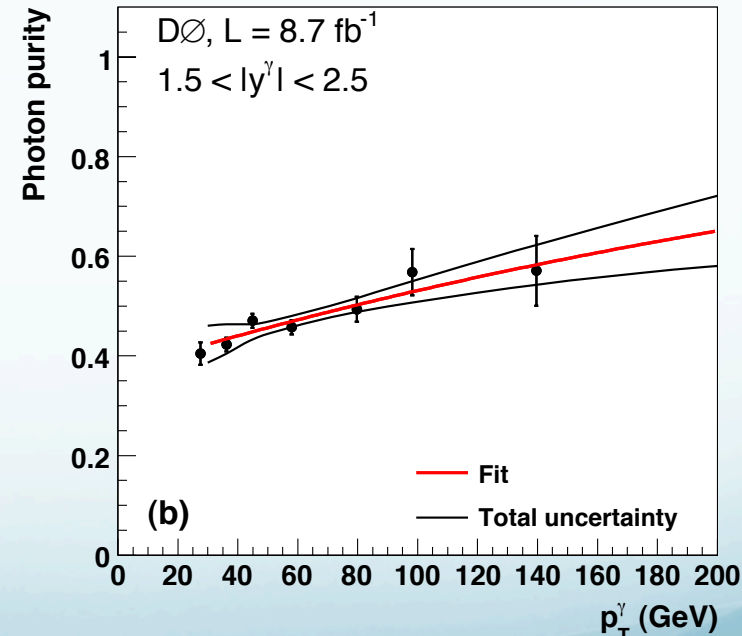
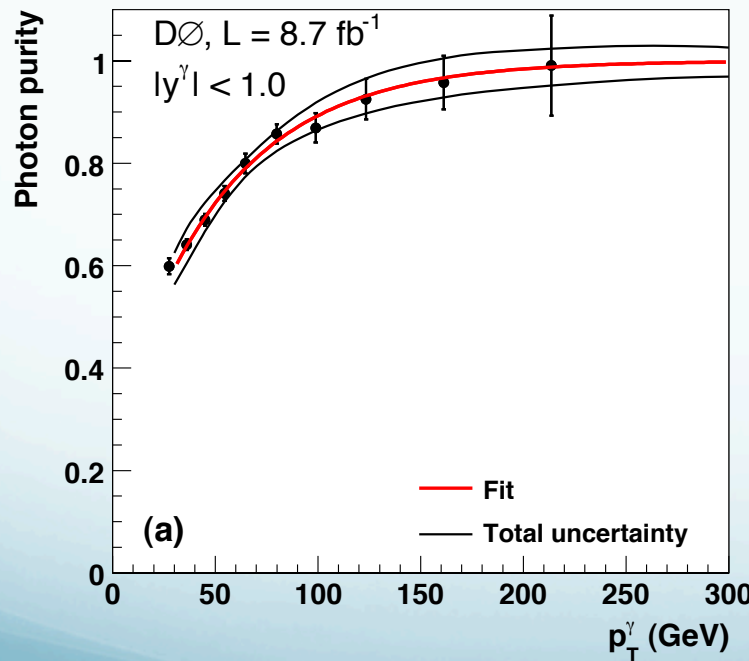


- Exploits differences in tracker, EM calorimeter and CPS activity between photons and jets, trained on MC
- Compared between γ and jets, describes data well
- ANN>0.3 is 98% efficient for photons

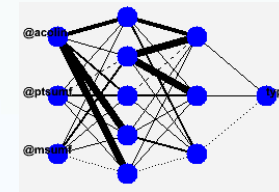


γ purities

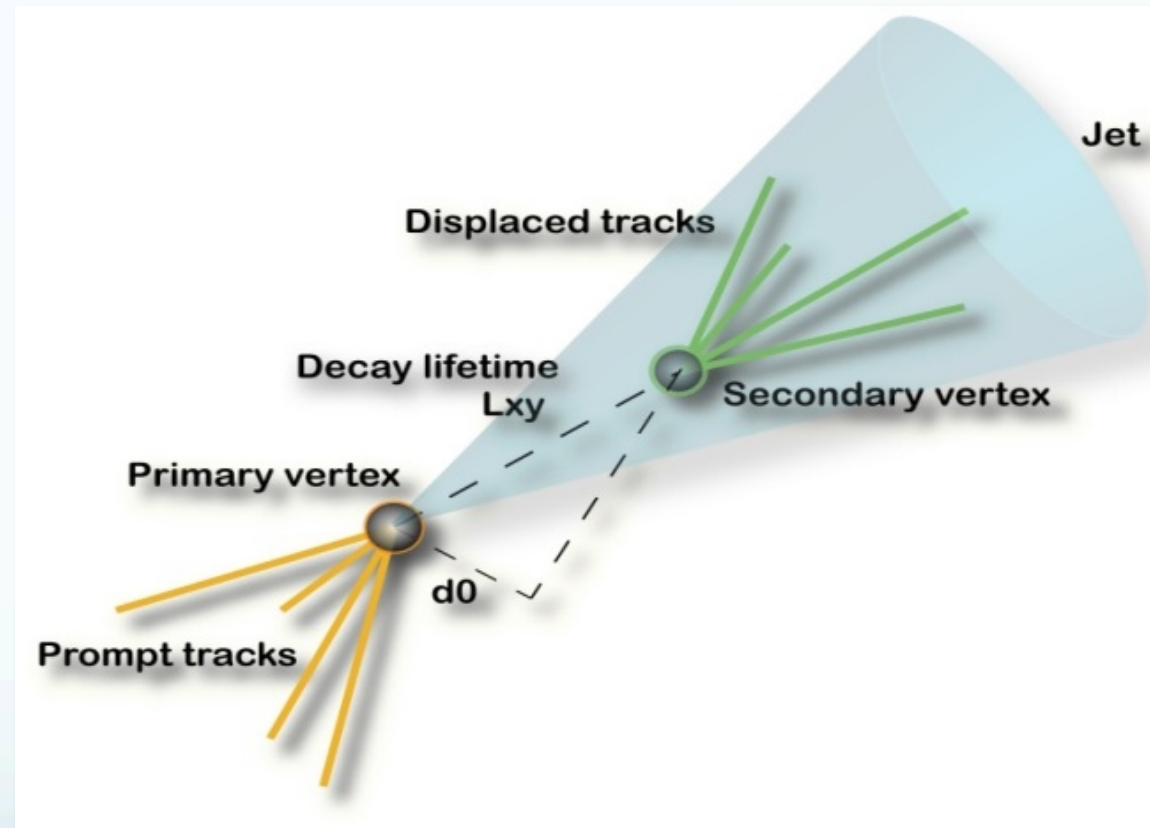
- $\gamma\gamma$ uses 4x4 matrix method (solving for $\gamma\gamma$, $\gamma + \text{jet}$, jet + γ , jet+jet fractions, particles p_T ordered)
- $\gamma+b$ uses bin-by-bin ANN template fit to data



B-jet ANN

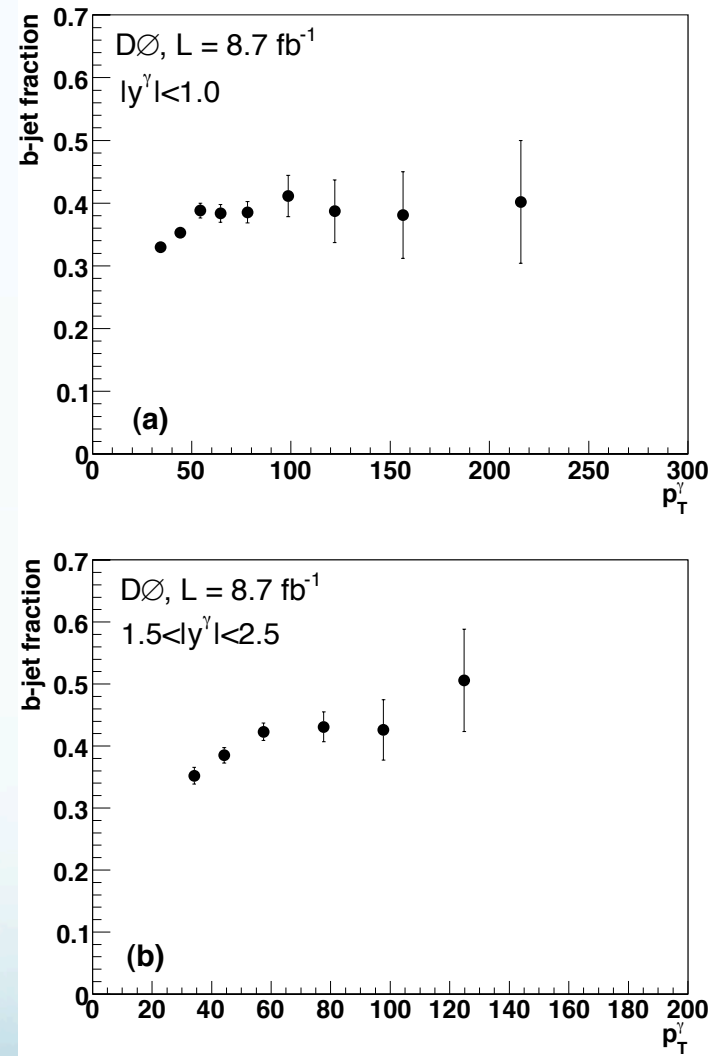
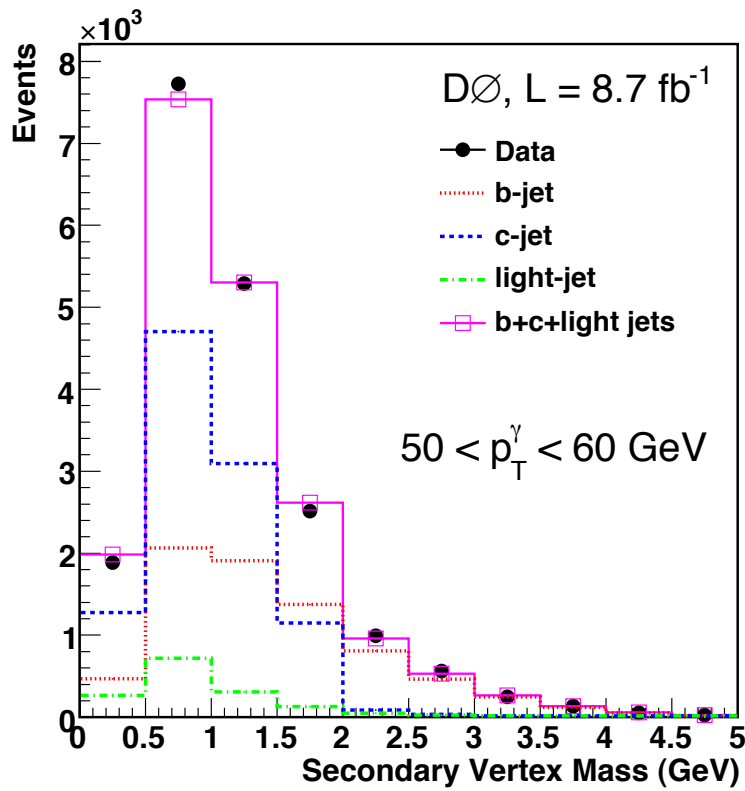


- Variables
 - Number of SV
 - Invariant mass of tracks, associated with SV (M_{SVT})
 - Number of tracks used to reconstruct SV
 - 2D decay length significance of the SV
 - Weighted combination of transverse IP significances
 - Probability of jet tracks to originate from PV



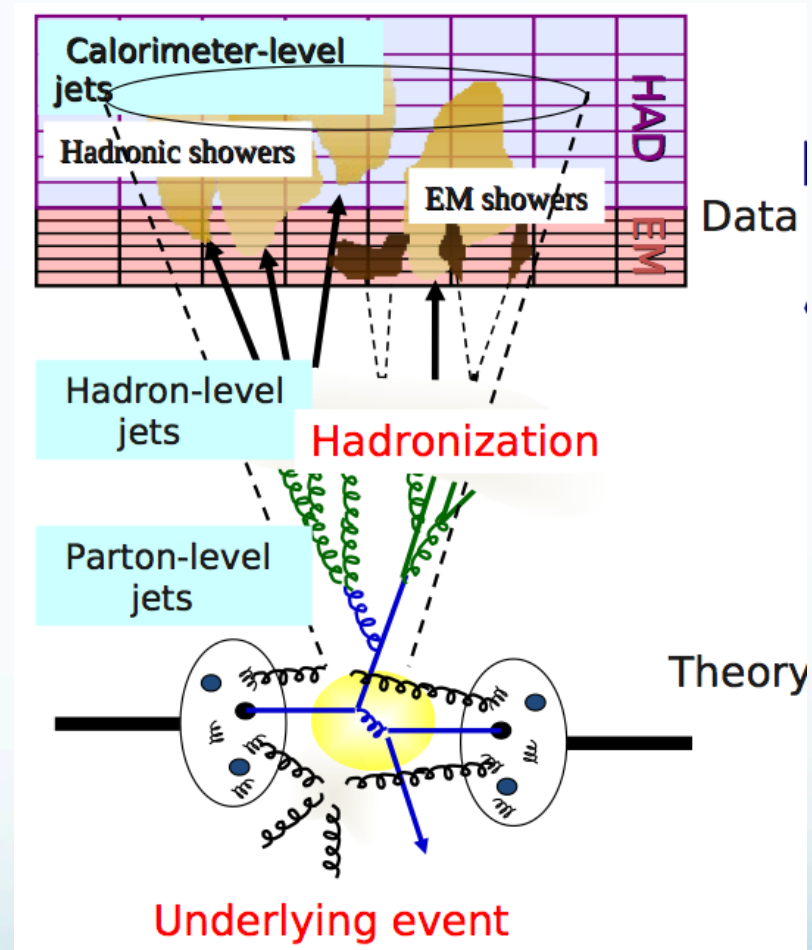
$\gamma + b$ b-jet fractions

- Bin-by-bin M_{SVT} template fit to data



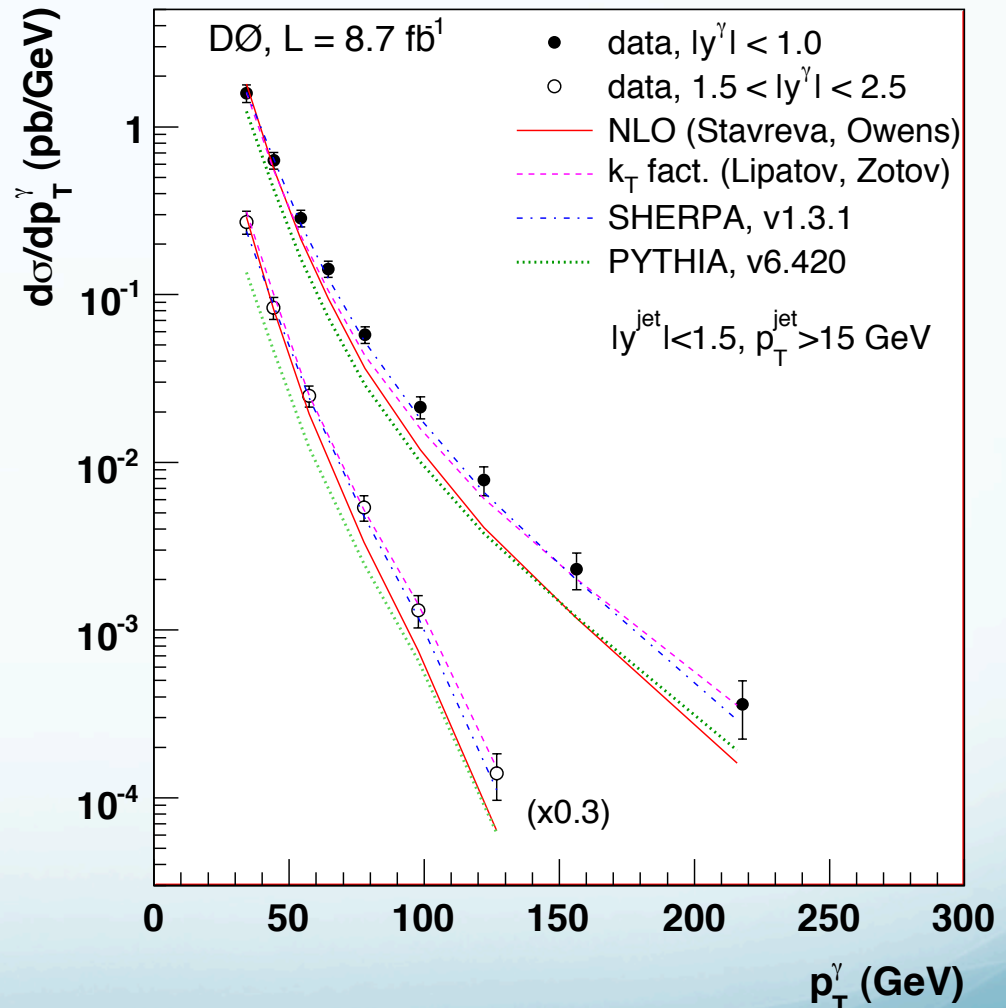
Compatibility corrections

- Theory (fixed order NLO) corrected to hadronization and multiple parton interactions
 - $\gamma + b$ 5-10% (2% uncert)
 - $\gamma \gamma$ 4-5.5% (0.5% uncert)
 - Calculated from Pythia tune A and S0 ($\gamma \gamma$)
 - Pythia tune A and Sherpa ($\gamma + b$)
 - Sherpa already has
- Data are corrected for detector effects, migrations and pileup, and presented at particle level



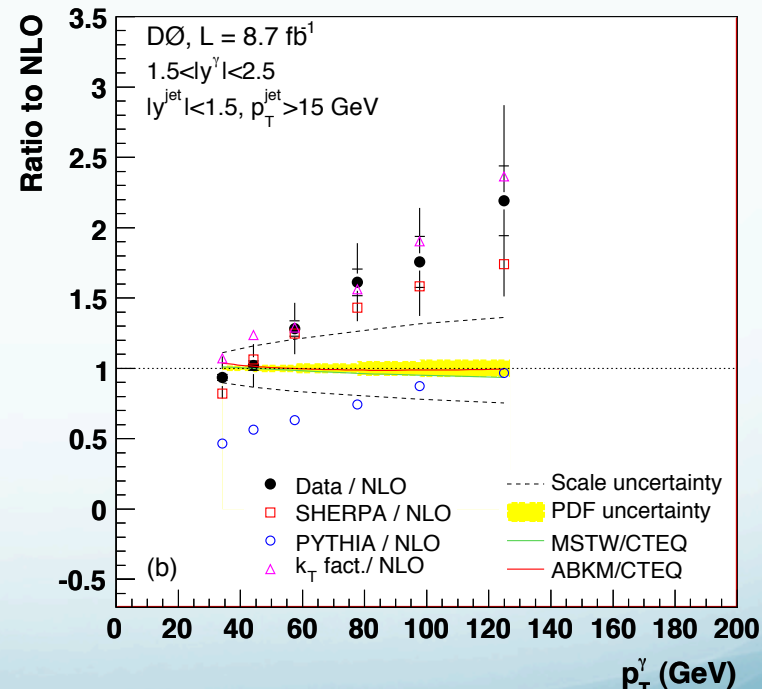
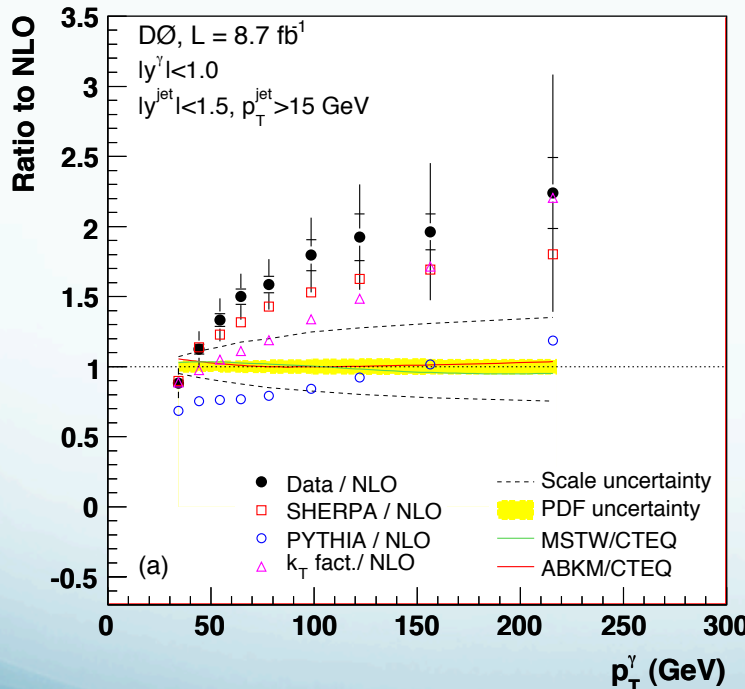
$\gamma + b$ cross sections

- Theory isolation PYTHIA and SHERPA particle level, NLO parton level
 - $E_T^{\text{iso}}(0.4) < 2.5 \text{ GeV}$
- NLO at factorization μ_F , fragmentation μ_f , renormalization scales $\mu_R = p_T^\gamma$
 - CTEQ6.6M
- k_T
 - Additional contributions due to integration over k_T^2 above scale μ^2 (additional gluon radiation)
- PYTHIA 2 \rightarrow 2 ME ($g \rightarrow bb$ in PS), CTEQ6.1L
- SHERPA ME $\gamma +$ up to 3 jets, at least 1 b-jet, 2nd hard jet in $g \rightarrow bb$
 - Resummation of further emissions



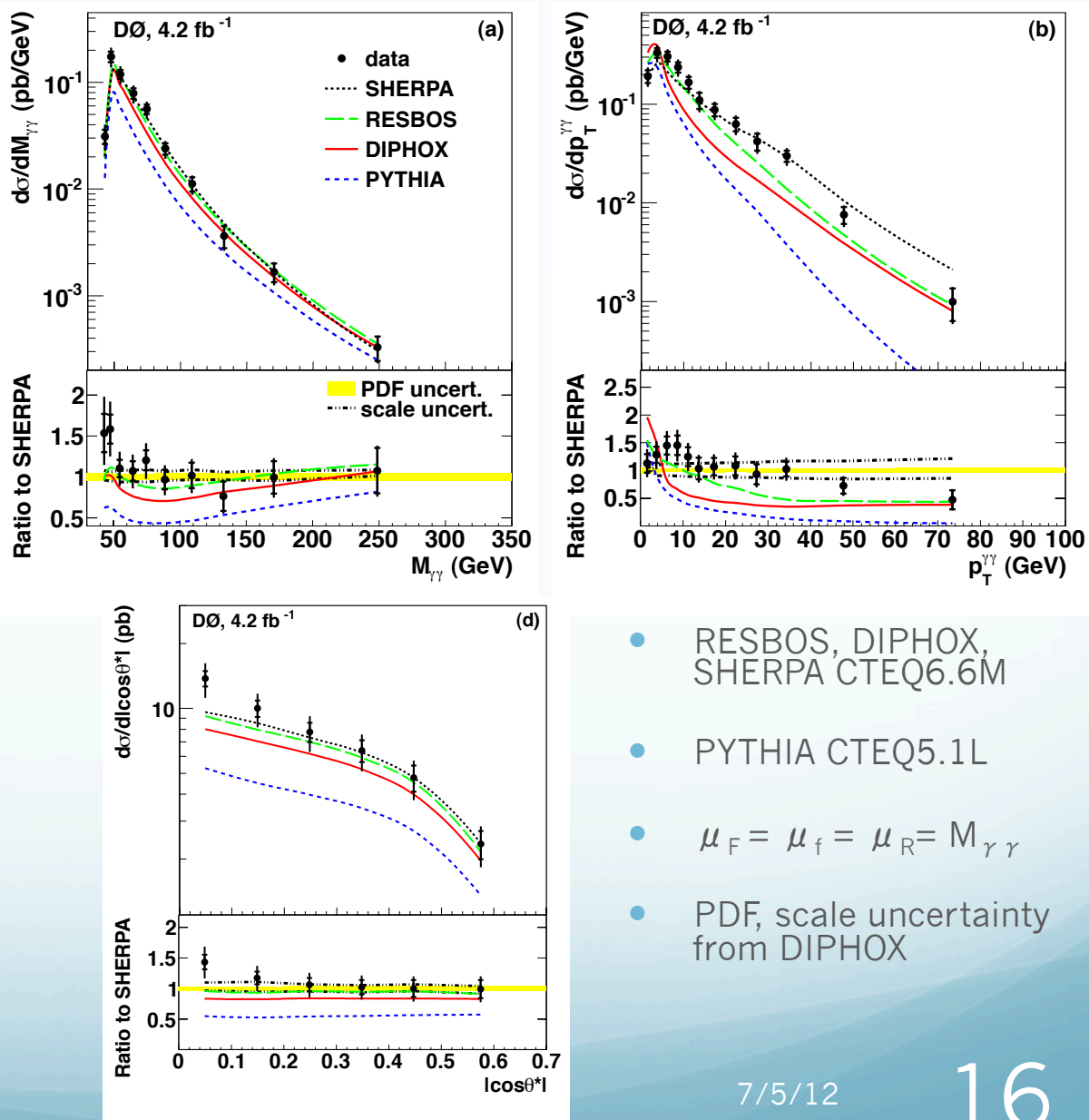
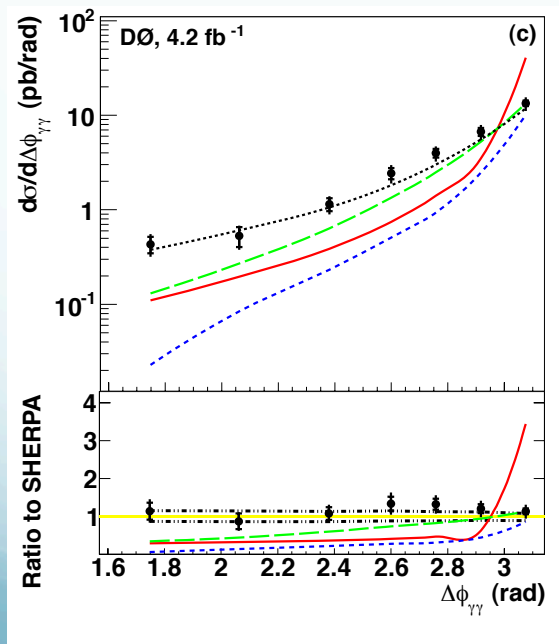
$\gamma + b$ ratios to NLO

- NLO agrees $30 < p_T^\gamma < 70$ GeV (within scale, PDF and experimental uncertainties), differs above
 - Needs higher order corrections for $q\bar{q} \rightarrow \gamma g$ ($g \rightarrow bb$)
- Best with SHERPA (allows 2 additional jets)



$\gamma\gamma$ single differential X-sections

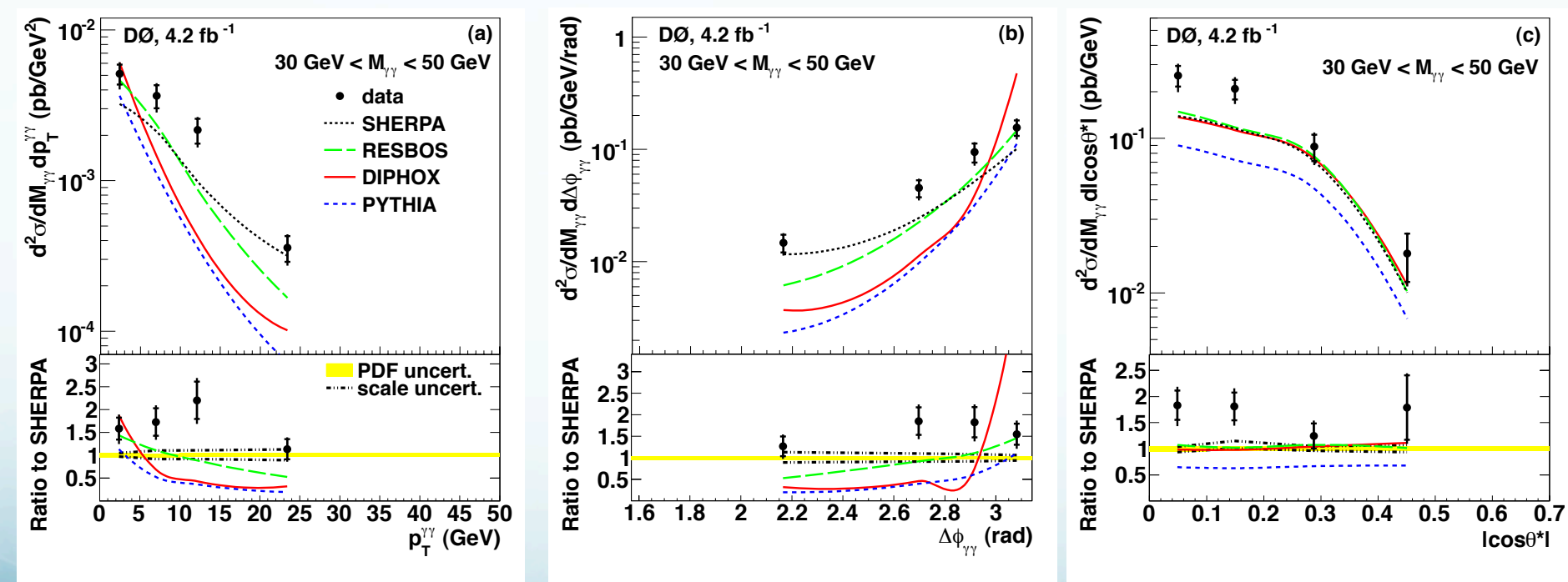
- $E_t^{\text{iso}}(0.4) < 2.5 \text{ GeV}$
 - Particle SHERPA, PYTHIA
 - Parton RESBOS, DIPHOX



$\gamma\gamma$ double differential X-sections

$30 < M_{\gamma\gamma} < 50 \text{ GeV}$

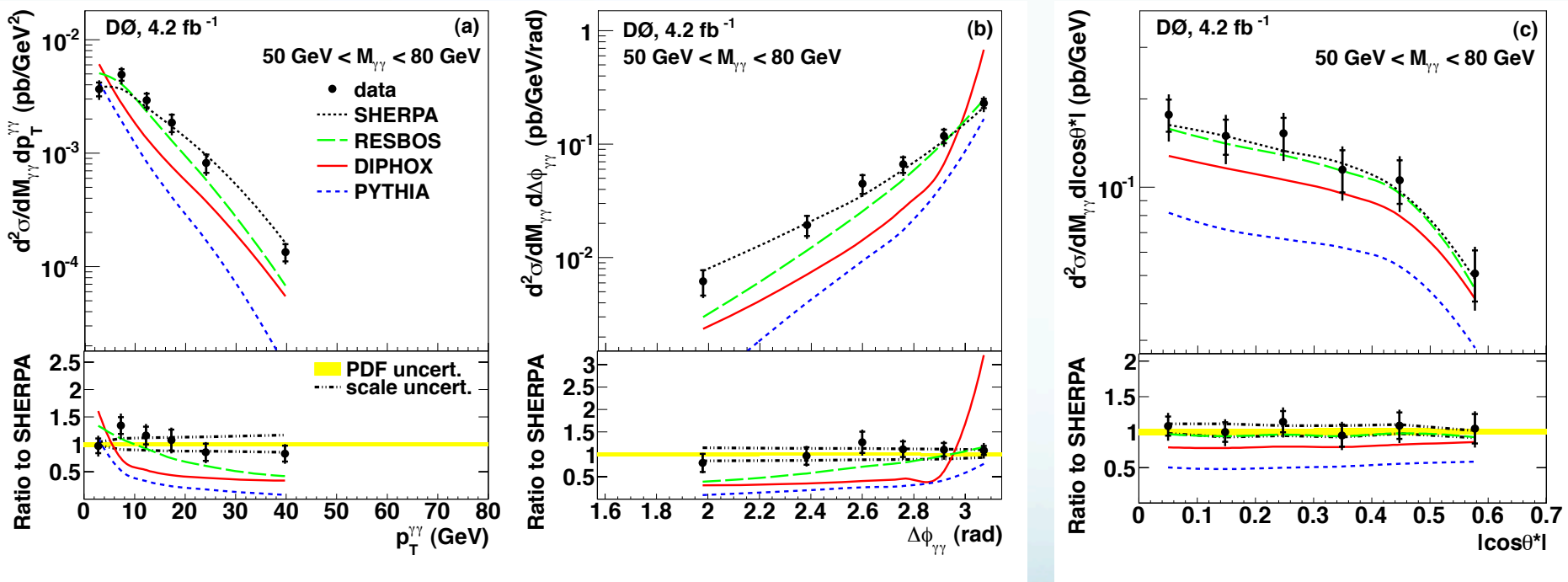
- Large discrepancies with RESBOS (used to correct for experimental effects, with acceptance reweightings to eliminate model dependence), SHERPA better



$\gamma\gamma$ double differential X-sections

$50 < M_{\gamma\gamma} < 80 \text{ GeV}$

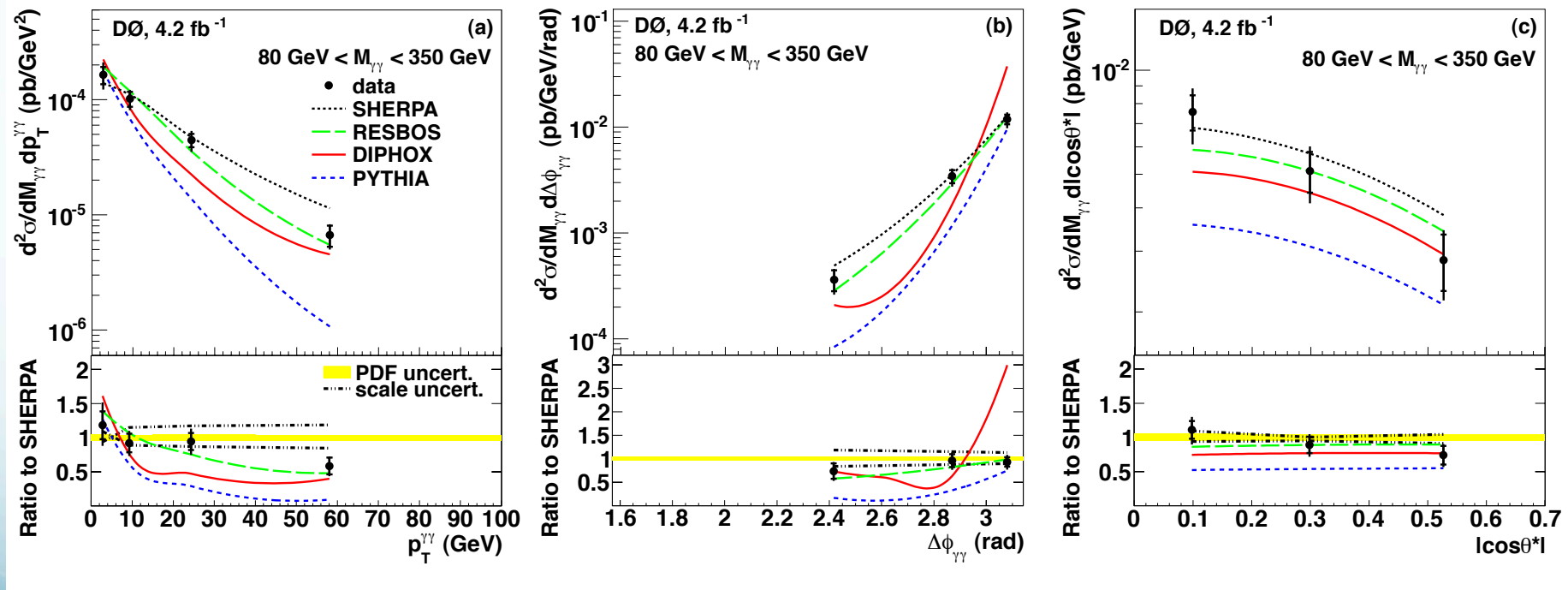
- Predictions agree better
- DIPHOX divergent at $\Delta\phi_{\gamma\gamma} \approx \pi$ (no resummation)



$\gamma\gamma$ double differential X-sections

$80 < M_{\gamma\gamma} < 350 \text{ GeV}$

- High mass SHERPA overshoots data at high $p_T^{\gamma\gamma}$



Summary

- Measured $\gamma+b$ differential x-sections vs p_T^γ
- Single differential $\gamma\gamma$ x-sections vs $M_{\gamma\gamma}$, $p_T^{\gamma\gamma}$, $\Delta\phi_{\gamma\gamma}$, $|\cos\theta^*|$
- Double differential $d^2\sigma/dp_T^{\gamma\gamma}dM_{\gamma\gamma}$, $d^2\sigma/d\Delta\phi_{\gamma\gamma}dM_{\gamma\gamma}$,
 $d^2\sigma/d|\cos\theta^*|dM_{\gamma\gamma}$ in 3 $M_{\gamma\gamma}$ bins
- Used high photon energy resolution to probe wide range of x ($0.007 < x < 0.4$) in $\gamma+b$
- Details of $\gamma\gamma$ shapes for fragmentation, new phenomena precision background x-section measurements, PDF effects
- NLO calculations miss higher order terms to describe effects in $q\bar{q} \rightarrow \gamma g$ ($g \rightarrow b\bar{b}$) at high p_T^γ , SHERPA describes those better by using extra jets in ME.
- RESBOS does not describe well the fragmentation effects at low $\Delta\phi_{\gamma\gamma}$, SHERPA again does a better job in describing higher order effects because of the match of PS and ME.